Building and Environment 296 (2026) 114483

Contents lists available at ScienceDirect

Building and Environment

journal homepage: www.elsevier.com/locate/buildenv

A mineral-based approach to cool asphalt pavements: Results from a field experiment

Fabrizio Orlando [a,*], Johannes Schindler [b], Peter Mikhailenko [b], Tobias Balmer [c], Philipp Hunziker [a], Joachim Schoelkopf [a]

[a] Omya International AG, Froschackerstrasse 6, CH-4622, Egerkingen, Switzerland
[b] Grolimund+Partner AG, Waldeggstrasse 42a, CH-3097, Liebefeld-Bern, Switzerland
[c] Weibel AG, Rehhagstrasse 3, CH-3018, Bern, Switzerland

ARTICLE INFO

Keywords:
Cool pavements
High-albedo asphalt
Reflective pavements
Urban heat island (UHI)
Ground Calcium Carbonate (GCC)
Reflective aggregates
Sustainable urban infrastructure

ABSTRACT

The Urban Heat Island (UHI) effect intensifies climate change challenges in cities, with asphalt pavements contributing significantly due to their low solar reflectivity and high heat retention. We conducted a comparative field experiment to quantify the cooling performance of reflective asphalt pavements in which the mineral fraction of the wearing course was fully replaced by highly reflective ground calcium carbonate (GCC) aggregates to increase pavement solar reflectance (albedo). Seven test sections (including untreated references) based on two asphalt mixtures and three types of post-laydown treatment were installed in a parking lot in Egerkingen, Switzerland, and monitored over a summer season in a real-world setting. Results indicate that embedded GCC aggregates significantly increase pavement albedo and reduce surface temperatures by up to 5 °C relative to the reference section. Across the tested configurations and conditions, we observed an approximately linear relationship between albedo and surface temperature, corresponding to an average cooling of ~6 °C per 0.1 increase in albedo. This on-site validation provides evidence-based performance quantification for a GCC-based, structurally integrated cool pavement approach and supports its potential as a scalable option for reducing pavement surface temperatures.

1. Introduction

Over the last decades, global temperatures have increased due to climate change, exposing populations to its severe impacts. Cities experience this warming particularly strongly: they often become much hotter than surrounding rural areas, a phenomenon known as Urban Heat Island (UHI) [1]. This effect is mainly caused by anthropogenic emissions as well as by rapid urbanization, which leads to a large increase in buildings, roads, and infrastructures at the expense of green areas. As a result, urban areas trap and store heat because man-made materials—especially dark surfaces like asphalt pavements—absorb and retain more energy than natural surfaces [2].

Rising urban heat poses significant health risks and environmental challenges. High temperatures increase the risk of heat-related illnesses [3], raise energy demand [4,5], and contribute to excess heat and air pollutant emissions [6], including greenhouse gases. As urbanization and climate change progress, UHI intensity is anticipated to increase, making mitigation strategies a central element of sustainable urban development. These include cool pavements [7] and cool roofs [8], expansion of urban green [9] and blue spaces [10], and climate-sensitive urban design [11–13], including enhanced rainwater retention [14]. Because more than 30% of urban surfaces are paved [15], most of which being asphalt, road surfaces are widely recognized as major contributors to UHIs [16–18]. Accordingly, cool pavements are considered a practical and effective mitigation strategy, particularly where alternative cooling options (e.g., green and blue infrastructure) are not feasible [19–22].

"Cool pavements" are paving materials or technologies designed to minimize heat absorption or enhance cooling relative to traditional pavements [23–25]. While pavement-scale surface cooling is well documented, effects on near-surface air temperature are less certain [26,27] and depend on the spatial extent and configuration of treated area. Neighborhood-scale deployments report modest but statistically relevant reductions in near-surface temperatures [20,21,26,27], and modeling suggests that kilometer-scale coverage may be required to produce a measurable temperature change at 2 m above ground [28–31]. Cool pavements are generally categorized into permeable and

* Corresponding author.
E-mail address: fabrizio.orlando@omya.com (F. Orlando).

https://doi.org/10.1016/j.buildenv.2026.114483
Received 1 December 2025; Received in revised form 2 March 2026; Accepted 13 March 2026
Available online 14 March 2026

reflective pavements. Permeable pavements allow water infiltration and promote evaporative cooling, whereas reflective pavements increase solar reflectance, i.e., albedo (α), thereby limiting radiative heat gain [23–25,32]. Both approaches can reduce surface temperatures substantially under favorable conditions, with additional co-benefits such as stormwater management and noise reduction for permeable systems, and limited risk of rutting and raveling for cooler surfaces [29–33]. However, permeable designs rely on moisture availability and may lose effectiveness due to clogging from debris, which reduces water infiltration and evaporative cooling, particularly in arid or maintenance-limited contexts [29,31].

Reflective pavements are designed to raise albedo—defined as the ratio of reflected (R) to incoming (I) solar energy: $\alpha = R/I$—so that less heat is absorbed and surface temperatures remain lower. High albedo is obtained either by applying reflective coatings or by embedding light-colored aggregates in the surface layer. Notably, albedo can be raised also by leveraging pigments selective to near-infrared radiation, thus increasing solar reflectivity with no change to surface appearance [30, 34–36].

Laboratory tests showed that painted asphalt can reduce surface temperature by up to 15 °C compared to untreated specimens [37]. Reflective coatings appear effective also on white concrete tiles [38], with cooling more pronounced under higher peak solar radiation [39]. This strong cooling potential is confirmed under extreme desert conditions, where coatings increased pavement albedo from 0.24 to 0.70 and lowered surface temperature from 60 °C to 47 °C [40]. However, field-scale pilots typically show more moderate, site-dependent cooling than laboratory benchmarks. In Phoenix, Arizona, treated asphalt surfaces were approximately 5.0 °C to 8.4 °C cooler than untreated asphalt concrete during peak hours [20], while a pilot program in San Antonio, Texas, reported average reductions of 2 °C relative to untreated control sites, with maximum reductions of 10 °C relative to new pavement [21].

However, reflective coatings may present limitations: glare and higher mean radiant temperature can cause pedestrians discomfort and raise heat loads in adjacent buildings [41], and performance can degrade as weathering, wear, and soiling reduce reflectivity [23,34]. Their typically short service life increases maintenance costs and associated environmental burdens. Life-cycle assessments report higher environmental impacts and flows than chip or slurry seals of similar thickness [42], often due to TiO_2 content, which increases embodied energy and cost compared to conventional aggregates.

An alternative approach to overcome the limitations of high-albedo coatings is to produce cool pavements using light-colored aggregates, which intrinsically exhibit high solar reflectivity. Chip-seals—in which asphalt binder is applied to an existing pavement and high-albedo aggregates are spread and rolled in—can initially reach near-aggregate albedo, but this typically declines with use and stabilizes after several years. Surface cooling of 4–6 °C per 0.1 albedo increase has been reported [43,44], and reinforced chip seals reduced temperatures by 12 °C versus conventional pavements [45]. Their drawbacks include higher placement complexity and cost than pre-mixed asphalt or slurry seals, as well as aggregate loss in high-shear (tight turning) and high-speed locations [43]. Other approaches include dosing hydrated lime onto freshly laid asphalt to produce a light-gray pavement which is about 3 °C cooler relative to conventional black asphalt [46]. Recent field trials in Switzerland investigated the use of bright flint aggregates to partially replace the standard mineral in both dense and porous asphalt. Particularly when combined with surface treatments, this approach reduced pavement surface temperatures by more than 6 °C [47,48]. In another similar approach, conventional aggregates were replaced with limestone in asphalt mixtures and combined with shot-blasting to remove the surface bitumen layer and expose the brighter aggregates. This treatment raised the albedo of new asphalt concrete from 0.08 to 0.20, but no corresponding reduction in surface temperature was reported [49].

Beyond these individual demonstrations, aggregate-based solutions offer a fundamental durability advantage. Unlike coatings, the reflectivity of asphalt pavements made with high-albedo aggregates is structurally integrated and therefore less prone to degradation, reducing the need for periodic reapplication [37,42]. With service lives of 5 to 20 years depending on local conditions, such pavements can lower maintenance costs and environmental footprint, making high-albedo aggregates a potentially cost-efficient option for sustainable urban applications [42]. Notably, the temporal evolution of albedo depends on cooling technology employed. Untreated or aggregate-enhanced asphalt surfaces often gain albedo as the binder oxidizes and aggregates become increasingly exposed [39,43,50,51], whereas surface-applied reflective coatings typically lose albedo over time due to soiling and weathering [23,34].

Despite this progress, field-scale evidence remains limited for mineral-based systems in which bright natural aggregates fully replace standard fractions across different asphalt types. Comparative evidence is also scarce regarding the effectiveness of practical post-laydown surface treatments designed to expose embedded bright aggregates. Moreover, a practical surface temperature–albedo relationship for mineral-based cool pavements to guide design and deployment is still lacking. Addressing these gaps requires side by side field sections representing relevant combinations of mixes and surface treatments, monitored through an initial weathering period against a consistent reference.

In response to these gaps, we conducted a field-scale evaluation of reflective cool pavements in which the mineral fraction of the wearing courses was entirely replaced by high-albedo ground calcium carbonate (GCC) aggregates. Two 8 mm asphalt mixtures were tested: Asphalt Concrete (AC), a conventional hot mix with regular bitumen, and Asphalt Concrete Macro Rough (AC MR), a deformation-resistant variant with higher macrotexture and polymer-modified bitumen (PmB). To expose bright aggregates and increase albedo, we applied three practical post-laydown surface treatments: water blasting, horizontal grinding, and gritting. The test sections were installed in a parking lot in Egerkingen, Switzerland, and monitored over a summer season in the absence of traffic to isolate the intrinsic albedo evolution. We measured albedo and surface temperatures relative to an untreated, fresh asphalt pavement as a reference, linking observed cooling to specific design variables. Albedo changes during the first season of natural weathering were tracked and related to corresponding surface temperature reductions. A linear dependence between surface temperature and albedo variation was established. These findings extend existing aggregate-based literature and are particularly relevant for parking lots and low-traffic streets, where GCC's mechanical properties and urban heat mitigation benefits are well aligned. Overall, this study advances a scalable implementation pathway: by fully embedding bright GCC into standard wearing courses, we demonstrate a practical route to structurally integrated reflectance validated at field scale. Durability and life-cycle performance are highlighted as key advantages to be substantiated through multi-year monitoring and a dedicated life-cycle assessment.

2. Experimental

2.1. Materials and methods

The high-reflectivity aggregates used in this study are a commercial-grade GCC of marble origin, supplied by Omya AG, Switzerland. The mineral was processed into two different particle size distributions tailored for use in AC and AC MR mixtures, in accordance with EN 13108–1 specifications. The measured CIELab color coordinates of the mineral are (97.7,0.0,1.0), indicating high brightness and almost neutral chromaticity.

The albedo of the aggregate was measured by evenly distributing about 15 kg of material on the ground, forming multiple layers that covered an area of 1 m^2. Measurements were performed using an albedometer consisting of two pyranometers (SP Lite2, by Kipp & Zonen): one oriented upward to measure incoming solar radiation, and

one oriented downward to measure reflected radiation from the surface at approximately 60 cm to minimize cosine-response errors and field-of-view contamination [52]. Measurements were carried out on sunny days to ensure consistent natural solar irradiation and minimize variability in the results [39].

Bitumen affinity of the aggregate was tested using the static method, which determines the degree of bitumen coverage on the mineral aggregate, as specified in EN 12697–11, index 5.4.7.

2.2. Field test layout

The test sections based on AC 8 and AC MR 8 mixtures cover an area of approximately 400 m^2 and were installed on June 19, 2024, in the parking area of Omya International AG in Egerkingen, Switzerland. Fig. 1 shows an aerial view of the experimental site, while the mix designs are reported in Table 1. Three post-laydown treatments were applied on July 5, 2024: water blasting (_wb), horizontal grinding (_gr), and gritting (_gt) (Fig. 2). Water blasting at high pressure (>2000 bar) removed the top bitumen layer and lightly eroded the mastic surrounding the larger grains, increasing texture. Grinding removed a thin surface layer of about 0.5–1 mm using a diamond tool, exposing the white aggregates more effectively but at higher risk of mechanical damage. Both processes ultimately exposed embedded GCC to increase surface reflectivity. In gritting, bright GCC aggregate was uniformly distributed on the freshly paved section and rolled in during compaction. A spreading density of approximately 700–800 g/m^2 ensures a

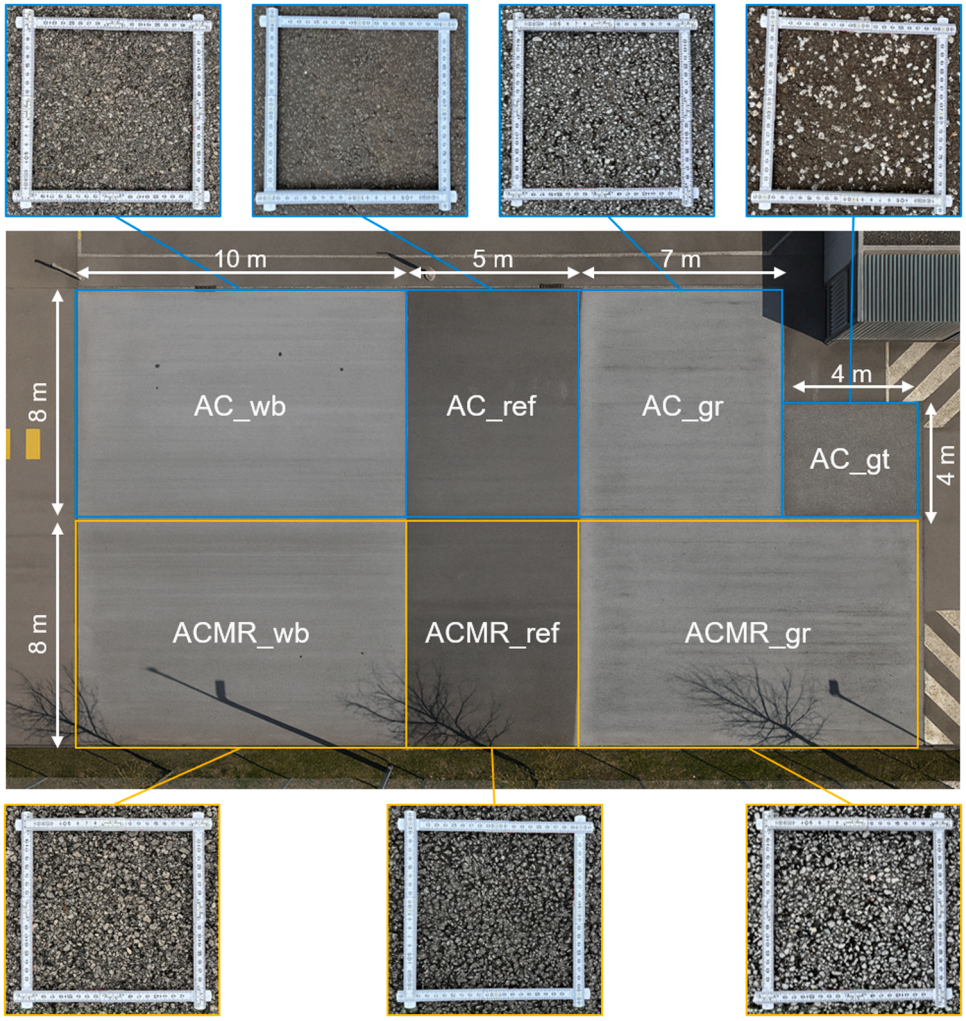

Fig. 1. Overview of test sections installed at the Omya International AG parking lot in Egerkingen, Switzerland, comparing AC and AC MR surfaces: untreated reference (_ref) and treated sections with water blasting (_wb), grinding (_gr), and gritting (_gt). Insets show close-up views of the surface textures for each section, taken at the end of the monitoring period (October 2, 2024).

Table 1
Mix designs and key characteristics of the AC and ACMR the test sections.

Test Section	Pavement Type	Aggregate and size fraction (mm)	Binder	Surface Treatment
AC_ref	AC 8	GCC_0/2 (38%), GCC_2/4 (10%), GCC_4/7 (42%), GCC_7/10 (10%)	B 50/70	None
AC_gr				Grinding
AC_wb				Water blasting
AC_gt				Gritting
ACMR_ref	AC MR 8	GCC_0/2 (18%), GCC_4/7 (61%), GCC_7/10 (21%)	PmB 45/80–65	None
ACMR_gr				Grinding
ACMR_wb				Water blasting

Fig. 2. Surface treatments applied to asphalt pavements: (left) grinding, (center) water blasting, and (right) gritting.

bright surface, while limiting aggregate clustering and loss of cohesion. Gritting was applied only to the AC mixture. Application parameters (e.g., water jetting and grinding passes) were held constant; hence, comparisons reflect treatment type rather than dose–response. Two sections were left untreated to serve as references (_ref), allowing natural weathering to gradually expose the bright aggregates. The layout ensured controlled monitoring conditions with consistent irradiance, minimal shadowing, and similar exposure to wind-induced cooling.

Surface temperatures were monitored using three calibrated, radiometric infrared (IR) cameras (thermoIMAGER TIM 40, by Micro-Epsilon) [53,54]. The cameras were mounted at 8 m height, each imaging a 3 × 3 m field and viewing the surface at angles >50° from a distance of approximately 10 m. The cameras automatically logged pixel-wise surface temperatures at 1-minute intervals. Each camera monitored three to four test sections, with overlapping fields of view at the boundaries between neighboring sections. Examples of thermograms are shown in Fig. S1a. Albedo was measured on July 9, 2024, and October 2, 2024, using the albedometer described above. For each test section, five measurements were collected from distinct areas at noon to maximize direct irradiance.

2.3. Data analysis

For each test section, specific regions of approximately 1.5–2 m^2 were defined within each IR image and their mean temperature was recorded at 1-minute intervals over the entire monitoring period. Outliers (e.g., objects with anomalous temperature) were removed and time series were smoothed by a running mean. The resulting temperature curves were then compared to identify the most representative area. The analysis time window was fixed at 12:00–16:00 to minimize shadow interference, capture the daily peak temperature, and ensure more consistent temperature differences between test sections. Nighttime data were excluded due to increased susceptibility to lateral heat flows in the absence of solar radiation.

Calibration was performed to correct systematic offsets between the IR cameras which may arise from the constant emissivity setting ($\varepsilon = 0.95$) applied consistently across all pavement sections (see SI). The estimated measurement uncertainty for surface temperature is ±0.5 °C, accounting for instrument specification and calibration repeatability. Additional details on calibration are provided in the SI. Importantly, the primary metrics of this study—(i) temperature differences between test sections measured simultaneously and (ii) the slope of the albedo–surface temperature relationship—are insensitive to absolute calibration bias, while between-camera non-uniform effects are addressed through cross-camera calibration and the stated uncertainty bounds (see SI).

Meteorological data from the MeteoSwiss station in Wynau [55] were used to identify hot, dry, and clear-sky days relevant for the analysis. Hourly conditions during two heat waves are summarized in Table S1. The ACMR_ref section consistently exhibited the highest temperatures throughout the monitoring and therefore served as the reference. The temperature effects for all other test sections were thus calculated as the difference between their respective temperature and that of ACMR_ref.

3. Results and discussion

3.1. GCC aggregate: evaluation of albedo, bitumen affinity and Los Angeles coefficient

Measuring the albedo of the mineral aggregates provides insights into their solar reflectivity and impact on surface temperature, key factors for optimizing cool pavements. The albedo of GCC was measured against two reference materials: a gray, high-quality split stone widely used in Swiss road construction, and bright flint used in an earlier cool pavement project in Switzerland [48]. Table 2 summarizes the albedo values of the raw aggregates measured as described in the methods. GCC exhibits a high albedo, comparable to the reference flint and clearly exceeding conventional split stone. This confirms the efficacy of bright GCC aggregates in reflecting solar radiation, thereby contributing to lower surface temperatures.

Bitumen affinity indicates binder-aggregate adhesion in asphalt mixtures, which is critical for the durability of road infrastructure. Table 2 presents adhesion results of pen-grade bitumen B70/100 with GCC and the reference split stone. The reference material exhibited an adhesion value of approximately 70%, consistent with values reported for minerals commonly used in Swiss road construction with unmodified bitumen. GCC achieved a coverage of 73%, indicating comparable or slightly superior affinity under identical conditions. Although this test is qualitative and influenced by factors such as bitumen type, GCC shows adhesion performance equivalent to the reference stone (under controlled conditions and using the same binder), suggesting a negligible risk of adhesion-related issues when incorporating this highly reflective aggregate into bituminous mixtures [56].

The Los Angeles (LA) coefficient quantifies resistance to impact and abrasion. A higher LA indicates a softer or more brittle material with lower resistance to crushing. Consequently, pavements containing aggregates with higher LA values are more prone to mechanical wear over their service life. For GCC, an LA value of 48 was measured. This exceeds Swiss specification limits for public roads (SN 670 103b), where aggregates for wearing courses typically require LA <25–30, depending on

Table 2
Albedo and bitumen affinity for GCC and other aggregate materials used in asphalt concrete pavements (aggregate size fraction: 2–4 mm).

Aggregate type	Albedo	Bitumen affinity (%)
GCC	0.32	73
Split stone	0.18	70
Flint	0.31	n.a.

load class. Nevertheless, GCC remains suitable for applications with less demanding mechanical requirements. These include walkways, public spaces, private parking areas, and other low-traffic zones, such as neighboring and residential roads, which represent primary use cases for cool pavement solutions.

3.2. Cool pavement demonstrator

3.2.1. Albedo response and aging

Fig. 3a shows the albedo measurements of the test sections at the beginning and end of the monitoring period. Several trends emerge.

First, surface treatments significantly increase pavement albedo. The untreated asphalt surfaces, AC_ref and ACMR_ref, exhibit the lowest albedos (0.08 and 0.07), consistent with values previously reported for freshly paved asphalt [39,48]. The ground sections, AC_gr and ACMR_gr, show the highest albedos (0.13 and 0.14), followed by the water-blasted sections, AC_wb and ACMR_wb (0.12 and 0.10).

Second, albedo increases over time. Measurements at the end of summer (October 2, 2024; patterned bars) are higher than at the start (July 9, 2024; filled bars). Ground and water-blasted AC surfaces reach albedos of 0.22 and 0.21, respectively, well above the AC_ref (0.13). Gritting also enhances albedo to 0.16. Corresponding AC MR values are slightly lower, with ACMR_gr (0.19) and ACMR_wb (0.18) both above the unmodified ACMR_ref (0.11). The enhanced reflectivity of the modified pavements results from removing black bitumen and exposing a brighter mineral surface. This effect is fully exploited when the mineral fraction is fully replaced with bright GCC. Notably, the measured albedo increase is mirrored by the visual brightening of the pavement surfaces, as shown in Fig. 3b–d.

Third, all AC surfaces consistently exhibit higher albedo values compared to their AC MR counterparts, regardless of the applied surface treatment. This is tentatively explained by the different macrotextures of the AC and AC MR courses, with the latter showing greater roughness, which reduces the reflection of solar radiation [31,57], thereby lowering the albedo.

The substantial increase in surface brightness over time is expected for asphalt pavements, driven by photocatalytic oxidation of bitumen (which transitions from black to light brown [58]) and processes that remove the binder and expose the aggregate [44], such as traffic-induced abrasion and weathering. The albedo increase over time has been documented in several studies on AC pavements. For example, Pomerantz et al. [43] reported albedo growth from 0.04 to around 0.12 over five years in the San Francisco East Bay. The broader study by Alleman et al. [50] reported increases from 0.04 to 0.15 over 15 years across several field tests in central and eastern U.S. cities. An albedo of 0.16 was measured for weathered AC pavements by Richard et al. [51], who proposed a logarithmic model to forecast albedo progression. Small test sections also show similar early increase in albedo occurring primarily within the first month after construction [39].

The albedo of the AC_ref and ACMR_ref sections measured at the end of the monitoring period already align with literature values for aged AC pavements [43,44,50,51], which is attributed to the bright aggregate that naturally becomes exposed, in addition to oxidative aging. Notably, these sections became significantly brighter after a short monitoring period—surpassing AC pavements aged over many years—indicating how quickly natural weathering can enhance reflectivity. Because the test sections were closed to traffic, the observed brightening is primarily due to early weathering and material-driven aggregate exposure rather

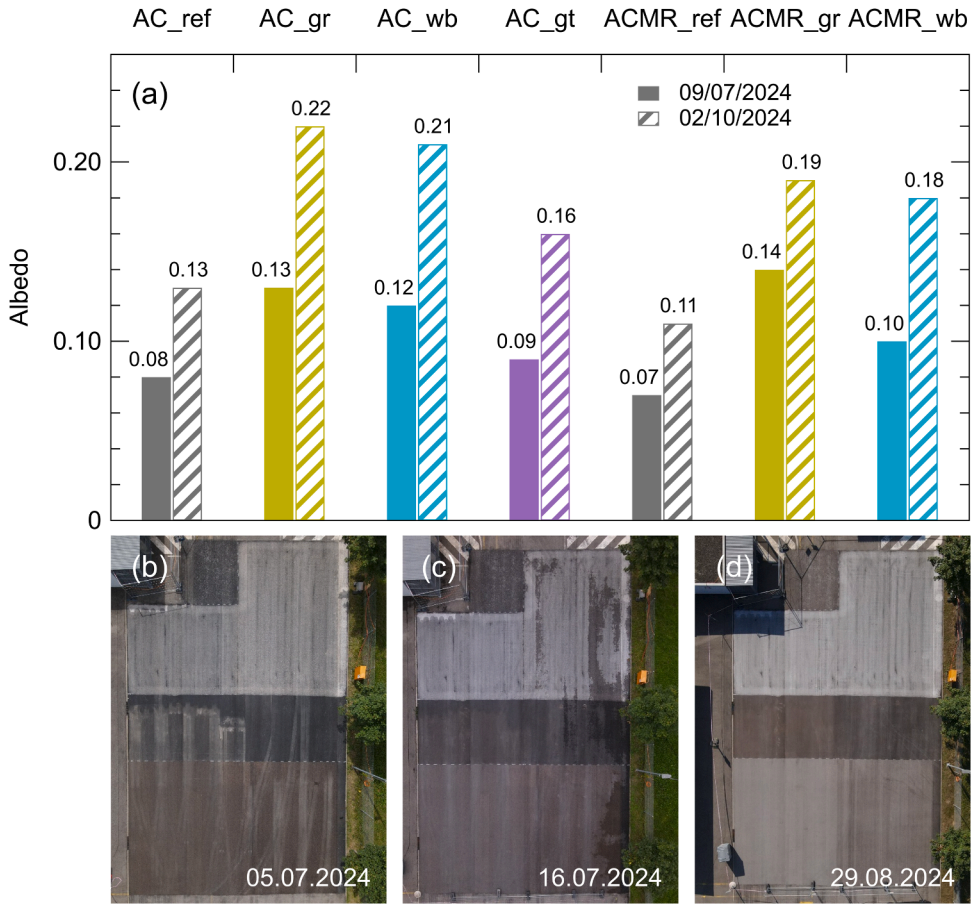

Fig. 3. (a) Average albedo of the test sections measured at the start (July 9, 2024) and end (October 2, 2024) of the monitoring period. (b–d) Aerial images showing the evolution of surface appearance over time. Note: images are rotated by 90 ° compared to Fig. 1.

than wear or contamination. In this context, a rough prediction can be made using the albedo model for AC pavements presented in Ref [50], which accounts for surface age and aggregate color. Applying this model to the present study—with aggregate grayscale between 224 and 255 and an offset matching an albedo of 0.21 (average of AC_gr and AC_wb in Fig. 3)—and accounting for both its standard deviation and the underestimation of albedo >0.15 [50], yields a predicted albedo exceeding 0.25 within two years of installation. This is unusually high compared to published values and approaches the range of 0.30–0.35, beyond which glare may become a concern [32]. It is important to note that in service, traffic may accelerate binder removal and aggregate exposure, but soiling (dust, traffic residues, oil) can offset brightening. Thus, the reported albedo values represent a low-soiling scenario; multi-season monitoring under real-world use is needed to quantify long-term performance retention.

3.2.2. *Cooling performance during monitoring and heat waves*

All test sections, particularly the unmodified AC_ref and ACMR_ref, exhibited significant temporal changes, complicating the choice of a stable reference. Notably, the ACMR_ref surface consistently showed the highest temperature and was therefore used as the baseline; all temperature differences are relative to ACMR_ref (see section 2.3, Data Analysis). Fig. 4 shows the average surface-temperature differences for (a) AC and (b) AC MR sections; panel (c) reports the average air temperature; panel (d) details the global radiation. The values in Fig. 4 represent daily averages calculated between 12:00 and 16:00 on warm and hot days, as defined in the experimental section.

The surface temperature assessment highlights the evolving thermal behavior of the test sections throughout the monitoring period. The temperature differences in Fig. 4a,b increase over time, indicating that these sections are becoming cooler relative to ACMR_ref. The most pronounced variations occur for AC_wb (−3.0 °C to −5.0 °C) and AC_gr (−3.5 °C to −5.2 °C). The trend is less pronounced for AC_gt, which closely resembles AC_ref, and for AC MR sections: ACMR_wb (−2.2 °C to −2.6 °C) and ACMR_gr (−3.9 °C to −4.1 °C). In general, a comparable evolution can be expected for AC_gt and AC_ref, given their similarity. Indeed, except for the areas topped with bright aggregates, AC_gt matches AC_ref. The rougher AC MR texture promotes shadowing and light trapping, reducing sensitivity to progressive brightening and thus yielding smaller temporal changes in both albedo (Fig. 3a) and temperature differences (Fig. 4b) compared to AC sections. In addition, rougher surfaces can retain binder in micro-depressions, delaying full exposure of bright aggregates compared to the denser, smoother AC surface.

It should be noted that as the reference ACMR_ref becomes progressively brighter—more than a standard fresh pavement—the measured temperature reductions would be even larger if a fresh standard asphalt were used as the reference. This indicates that the calculated cooling performance may underestimate the actual potential benefits.

To better illustrate the efficacy of cool pavements, data were analyzed over two distinct heat waves (HWs): August 10–13, 2024

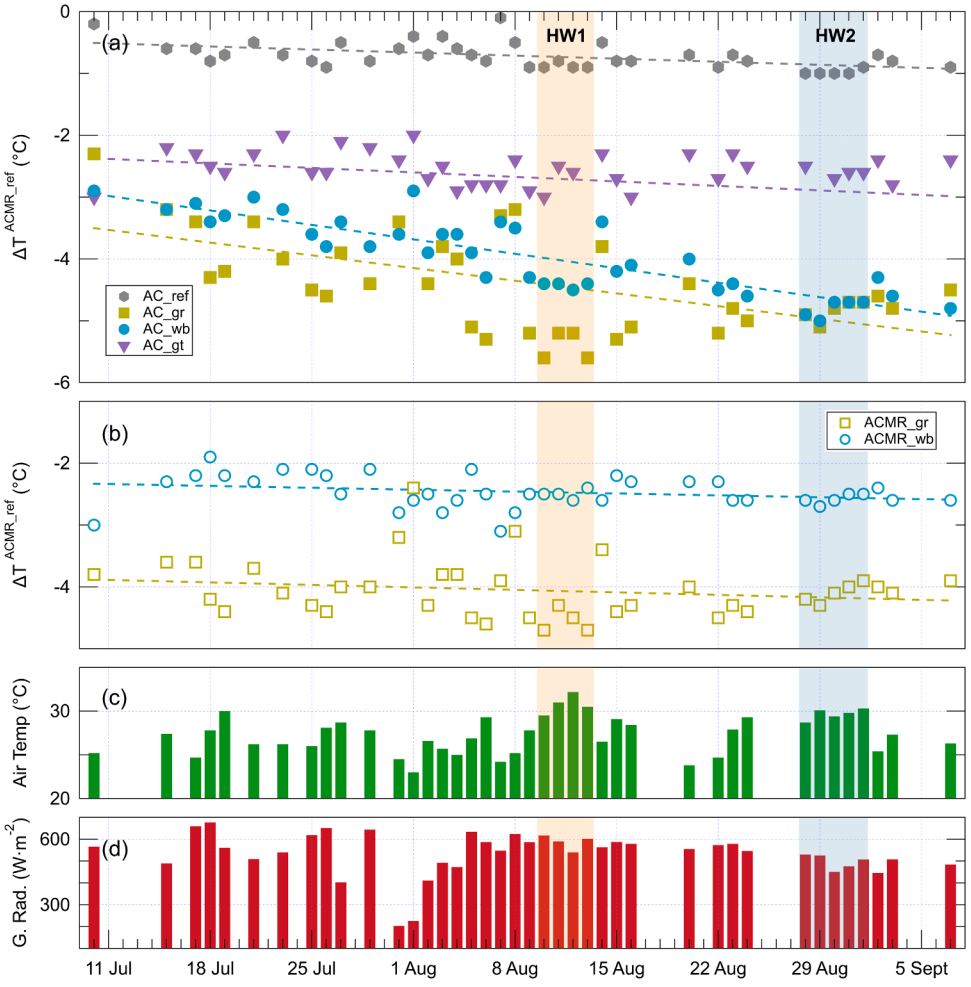

Fig. 4. Average temperature differences of (a) AC and (b) AC MR test sections relative to ACMR_ref during the monitoring period, with corresponding (c) air temperature and (d) global solar radiation. Values represent averages from 12:00 to 16:00 on warm and hot days. Only meteorologically relevant days are shown (see section 2.3, Data Analysis, for details).

Table 3
Average temperature reduction relative to ACMR_ref (ΔT_{av}) and maximum surface temperature (T_{Max}) for AC and AC MR test sections during two heat waves: HW1 (August 10–13, 2024) and HW2 (August 28–September 1, 2024).

Test section	Heat Wave 1 (August 10–13, 2024)		Heat Wave 2 (August 28–September 1, 2024)	
	ΔT_{av} (°C)	T_{Max} (°C)	ΔT_{av} (°C)	T_{Max} (°C)
AC_ref	−0.9 ± 0.1	55.6	−1.0 ± 0.1	50.5
AC_gr	−5.4 ± 0.2	51.2	−4.9 ± 0.1	46.6
AC_wb	−4.4 ± 0.1	52.3	−4.9 ± 0.1	46.7
AC_gt	−2.8 ± 0.3	54.0	−2.6 ± 0.1	48.7
ACMR_ref	-	56.5	-	51.4
ACMR_gr	−4.6 ± 0.2	51.9	−4.1 ± 0.2	47.4
ACMR_wb	−2.5 ± 0.1	54.3	−2.6 ± 0.1	49.1

(HW1), and August 28–September 1, 2024 (HW2). The results, including peak temperature and average temperature reduction relative to ACMR_ref are detailed in Table 3. Consistent with Fig. 4, the largest cooling effect is achieved on the ground sections: AC_gr, 5.4 °C (4.9 °C), and ACMR_gr, 4.6 °C (4.1 °C), in HW1 (HW2). These values are only slightly lower than those reported in pilot field applications using commercial cool coatings in Phoenix [20] and San Antonio [21]. Although it is challenging to compare studies that differ in technology, methodology, and site conditions, we note that the two US cities experience approximately 78% and 47% higher irradiance than Egerkingen [59]. The higher exposure enhances the effectiveness of high-albedo surfaces in reducing surface temperature and may explain the slightly lower performance observed in this study. Overall, these observations underscore the critical influence of geographic location and solar exposure on the performance of cool pavements.

High-pressure water blasting performed similarly to grinding on AC but less effectively on AC MR, with cooling of approximately 2.5 °C during both heat waves. Surface gritting, although less impactful, still achieved a significant temperature reduction of approximately 2.7 °C. As shown in Table 3, trends in average reductions mirror peak temperatures. Notably, HW2 maxima are lower than HW1, with differences ranging from 4.5 °C to 5.6 °C. This is explained by the slightly cooler conditions during HW2, as confirmed by lower air temperature and global solar radiation values (Fig. 4c,d). This may explain why, despite albedo increases over time, HW2 temperature reductions are not larger than in HW1: enhanced reflectivity in HW2 was offset by reduced irradiance [39].

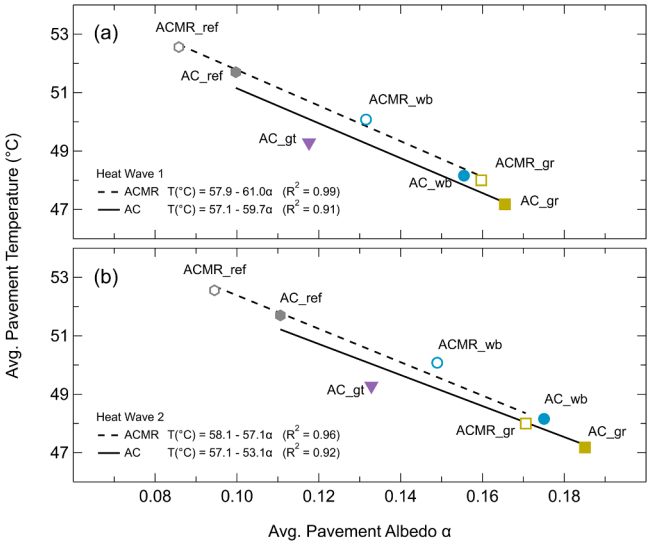

Fig. 5. Relationship between average surface temperature and albedo for AC and AC MR test sections during HW1 (August 10–13, 2024) and HW2 (August 28–September 1, 2024). Linear fits indicate cooling of approximately 6.0 °C and 5.5 °C per 0.1 albedo increase for HW1 and HW2, respectively. Fit equations and R^2 are shown in each panel. The fits are applicable within the albedo range and heat-wave conditions covered by the tested sections.

3.2.3. *Albedo–temperature scaling and implications*

Fig. 5 shows the average surface temperatures of the test sections plotted against their albedo. As albedo was not measured during the heat waves, the values shown in Fig. 5 are linearly interpolated from those in Fig. 3 at the corresponding time points. A linear fit reveals a cooling of about 6.0 °C and 5.5 °C for every 0.1 increase in albedo during HW1 and HW2, respectively. This slope is a local empirical fit and should be interpreted only within the albedo range and conditions covered in this study (α ~ 0.07–0.22; hot, sunny summer days; 12:00–16:00). Outside this domain, the surface temperature response is constrained by the full surface energy balance and should not be assumed to remain linear. Also, because regression slopes are invariant to uniform temperature offsets, the estimates in Fig. 5 are insensitive to absolute calibration bias. The slightly better cooling performance during HW1 is consistent with higher solar irradiance than in HW2. Although this simplified model does not account for surface texture, convective cooling, or lateral heat exchange between test sections and surrounding materials, the results clearly indicate that increasing albedo lowers surface temperature. The magnitude aligns with previously reported values for chip seals and AC pavements (between 2 °C and 5 °C per 0.1 increase in albedo) [43,44,60], supporting consistency with established radiative principles. The key distinction is structural: embedding bright GCC throughout the wearing course makes reflectance intrinsic and more persistent than in chip seals (aggregate-loss risks) or thin-layer reflective coatings. Differences in absolute temperature across studies are expected to scale with local global horizontal irradiance (GHI). Additionally, observed differences between visually similar surfaces may partly arise from wavelength-dependent reflectance (e.g., visible and near-infrared). Band-resolved data were not collected, as spectrally-resolved analysis is beyond the scope of this study.

AC MR test sections consistently exhibit higher surface temperatures than corresponding AC surfaces. A strong correlation between albedo and surface temperature is observed for both types of pavements. Together, these observations suggest that the rougher AC MR surface allows light to penetrate deeper, increasing the likelihood of absorption. This causes a decrease in reflectance and, consequently, albedo. Thermal conductivity and volumetric heat capacity may also contribute to the higher temperature of the AC MR pavement. The steeper aggregate gradation relative to AC likely increases air void content, reducing both thermal conductivity and heat storage capacity [61,62]. This may limit heat dissipation to deeper layers, causing the AC MR surface to retain energy and remain warmer under the same input than AC.

The findings presented in this study show that combining bright GCC aggregates with surface treatments significantly reduces surface temperatures, a mechanism relevant to UHI mitigation. The varying degrees of temperature reductions across test sections underscore the importance of considering surface texture and material composition in the design and application of cool pavements. In absolute terms, grinding yielded the largest albedo gains and surface temperature reductions, followed by water blasting. This difference likely stems from the gentler

nature of water blasting, which cannot remove bitumen that has inevitably penetrated the aggregate; it should be noted that increasing blasting pressure would primarily accelerate erosion rather than brightening. The effect appears more pronounced on rougher surfaces, as suggested by the larger albedo gap between water-blasted and ground AC MR sections compared to AC (Fig. 3). These differences diminished by the end of the test period, suggesting that weathering gradually wears away the residual surface bitumen. Gritting also performed well, highlighting the critical role of aggregate brightness in enhancing albedo, since increased reflectivity derives solely from the topping stones. Cooling performance of the grit surface could be further improved by increasing the coverage of topping stones, but durability may suffer due to increased stone-to-stone contact. In an end-use scenario, identifying an optimal balance between cooling efficiency and durability is essential and may vary depending on the intended use of the pavement, such as a low-traffic residential street or a parking lot.

Finally, we note operational considerations such as friction must be verified in service. Although skid-resistance implications of the post-treatments were not assessed in this study, we note that grinding and high-pressure water blasting are established retexturing techniques that, when applied within specification on suitable pavement types, generally preserve or even improve pavement friction [63–65].

4. Conclusions

This study demonstrates that incorporating bright GCC aggregates into asphalt mixtures, combined with targeted surface treatments, can effectively enable reflective cool pavements for urban applications, particularly parking lots and residential roads. Their impact on pavement albedo and surface temperature was quantified through field testing and monitoring over time.

The results confirm a significant increase in pavement albedo—up to 0.12 higher than untreated asphalt—for all surfaces containing bright GCC aggregates. This increase translated into substantial surface temperature reduction. The effectiveness of the applied treatments varied depending on both the asphalt mix design and the treatment type. On average, dense AC 8 courses achieved a slightly superior cooling performance to more porous AC MR 8 courses. By the end of the monitoring period, ground and water-blasted AC pavements showed comparable reductions of approximately 5 °C. The AC grit achieved about 2.5 °C of cooling with simpler implementation and lower cost. The smaller reductions measured on AC MR sections—approximately 4 °C (ground) and 2.5 °C (water-blasted)—are attributed to their higher macrotexture compared to AC. Overall, the findings indicate an average cooling of nearly 6 °C for every 0.1 increase in albedo—a slope that lies within the upper range reported for field studies, consistent with established radiative principles.

The observed increase in albedo during the three-month monitoring period, despite the absence of wearing factors such as vehicles or pedestrians, underscores the importance of asphalt mixture composition, specifically the full replacement of standard mineral fractions with bright GCC aggregates. Because asphalt tends to lighten as binder oxidizes and aggregates become exposed, albedo may continue to increase under low-soiling conditions. However, the long-term evolution in service will depend on local use and environment, including soiling (dust, traffic residues, oil contamination) and binder-related effects (e.g., bleeding) that can reduce reflectance. Accordingly, monitoring across several seasons under real traffic and a maintenance regime is needed to quantify albedo retention. If albedo is retained, or continues to rise, under service conditions, the technology could deliver greater cooling performance over time; these durability aspects are being assessed through ongoing and future monitoring.

Beyond performance and durability, practical deployment is also governed by material supply constraints. Since pavement aggregates are generally sourced locally, the feasibility of cool pavement designs is often limited by the regional availability of reflective aggregates. Demonstrating cool asphalt pavements using widely available GCC aggregates therefore expands deployment potential in regions where such materials are accessible.

From a sustainability perspective, integrating naturally occurring and widely available bright GCC directly into the asphalt mixture makes the cooling effect intrinsic to the pavement structure, potentially eliminating the need for synthetic coatings and their associated life-cycle concerns. When deployed at sufficient scale, GCC-based cool pavements may contribute to urban-heat mitigation and remain environmentally and economically viable over the long term. Because this study focuses on pavement-scale surface temperatures and albedo, translating these effects to neighborhood-scale near-surface air temperature requires modeling at appropriate spatial extent. Urban-climate modeling could be applied to estimate air temperature impacts under local conditions.

CRediT authorship contribution statement

Fabrizio Orlando: Writing – review & editing, Writing – original draft, Supervision, Investigation, Conceptualization. **Johannes Schindler:** Writing – review & editing, Investigation, Formal analysis, Conceptualization. **Peter Mikhailenko:** Writing – review & editing. **Tobias Balmer:** Writing – review & editing, Conceptualization. **Philipp Hunziker:** Writing – review & editing, Supervision. **Joachim Schoelkopf:** Writing – review & editing, Supervision.

Declaration of competing interest

Fabrizio Orlando, Philipp Hunziker, and Joachim Schoelkopf are employed by Omya International AG. Johannes Schindler, Peter Mikhailenko, and Tobias Balmer received compensation from Omya International AG for services related to installation and monitoring of the cool pavement test sections. This financial support did not influence the design, execution, or interpretation of the studies presented in this article.

Acknowledgments

The authors gratefully acknowledge Erik Bühlmann (Grolimund+Partner AG) for his expert consultation on the cool pavement test sections and Cathy Ridgway (Omya International AG) for her meticulous proofreading of the manuscript.

Supplementary materials

Supplementary material associated with this article can be found, in the online version, at doi:10.1016/j.buildenv.2026.114483.

Data availability

Data will be made available on request.

References

[1] EPA, U.S., Reducing Urban Heat islands: Compendium of Strategies, E.P. Agency, 2012. Editor.
[2] A. Mahdavi, K. Kiesel, M. Vuckovic, Methodologies for UHI analysis, in: F. Musco (Ed.), Counteracting Urban Heat Island Effects in a Global Climate Change Scenario, Springer International Publishing: Cham, 2016, pp. 71–91. Editor.
[3] N. Nazarian, et al., Integrated assessment of urban overheating impacts on Human life, Earths. Future 10 (8) (2022) e2022EF002682.
[4] M. Santamouris, et al., On the impact of urban climate on the energy consumption of buildings, Sol. Energy 70 (3) (2001) 201–216.
[5] C. Guattari, L. Evangelisti, C.A. Balaras, On the assessment of urban heat island phenomenon and its effects on building energy performance: a case study of Rome (Italy), Energy Build. 158 (2018) 605–615.
[6] C. Sarrat, et al., Impact of urban heat island on regional atmospheric pollution, Atmos. Environ. 40 (10) (2006) 1743–1758.

[7] H. AzariJafari, et al., Urban-scale evaluation of cool pavement impacts on the Urban heat island effect and Climate change, Environ. Sci. Technol. 55 (17) (2021) 11501–11510.
[8] K. Bamdad, Cool roofs: a climate change mitigation and adaptation strategy for residential buildings, Build. Environ. 236 (2023) 110271.
[9] N.H. Wong, et al., Greenery as a mitigation and adaptation strategy to urban heat, Nat. Rev. Earth Environ. 2 (3) (2021) 166–181.
[10] L. Fricke, R. Legg, N. Kabisch, Impact of Blue Spaces on the Urban Microclimate in Different Climate zones, Daytimes and Seasons – A systematic Review, 101, Urban Forestry & Urban Greening, 2024 128528.
[11] M. Georgescu, et al., Urban adaptation can roll back warming of emerging megapolitan regions, Proc. Natl. Acad. Sci. 111 (8) (2014) 2909–2914.
[12] S. Lenzi, J. Sádaba, A. Retegi, Climate adaptation in urban space: the need for a transdisciplinary approach, Front. Sustain. Cities. 7 (2025). **Volume - 2025**.
[13] A. Yiannakou, K.-D. Salata, Adaptation to climate change through spatial planning in compact urban areas: a case study in the City of Thessaloniki, Sustainability 9 (2) (2017).
[14] J. Xu, et al., Urban rainwater utilization: a review of management modes and harvesting systems, Front. Environ. Sci. 11 (2023). **Volume - 2023**.
[15] H. Akbari, L.Shea Rose, H. Taha, Analyzing the land cover of an urban environment using high-resolution orthophotos, Landsc. Urban. Plan. 63 (1) (2003) 1–14.
[16] C.G. Hoehne, et al., Valley of the sun-drenched parking space: the growth, extent, and implications of parking infrastructure in Phoenix, Cities. 89 (2019) 186–198.
[17] C.G. Hoehne, et al., Urban heat implications from parking, roads, and cars: a case study of Metro Phoenix, Sustain. Resilient. Infrastruct. 7 (4) (2022) 272–290.
[18] M. Shamsaei, A. Carter, M. Vaillancourt, Using construction and demolition waste materials to alleviate the negative effect of pavements on the urban heat island: a laboratory, field, and numerical study, Case Stud. Constr. Mater. 20 (2024) e03346.
[19] T. Asaeda, V.T. Ca, A. Wake, Heat storage of pavement and its effect on the lower atmosphere, Atmos. Environ. 30 (3) (1996) 413–427.
[20] F.A. Schneider, et al., Evidence-based guidance on reflective pavement for urban heat mitigation in Arizona, Nat. Commun. 14 (1) (2023) 1467.
[21] N. Debbage, et al., Evaluating the performance of cool pavement in San Antonio, Texas as an urban heat mitigation measure, J. Appl. Meteorol. Climatol. (2025).
[22] X. Gong, et al., A systematic review on the strategies of reducing asphalt pavement temperature, Case Stud. Constr. Mater. 18 (2023) e01852.
[23] Y. Wardeh, et al., Review of the optimization techniques for cool pavements solutions to mitigate Urban Heat Islands, Build. Environ. 223 (2022) 109482.
[24] Z. Wang, et al., Materials to mitigate the Urban heat island effect for cool pavement: a brief review, Buildings 12 (8) (2022) 1221.
[25] S. Kappou, et al., Cool pavements: state of the art and new technologies, Sustainability. 14 (9) (2022) 5159.
[26] J. Ko, et al., Measuring the impacts of a real-world neighborhood-scale cool pavement deployment on albedo and temperatures in Los Angeles, Environ. Res. Lett. 17 (4) (2022).
[27] D. Elgendy, O. Tolba, T. Kamel, The impact of increasing urban surface albedo on outdoor air and surface temperatures during summer in newly developed areas, Sci. Rep. 15 (1) (2025) 25165.
[28] D. Millstein, R. Levinson, Preparatory Meteorological Modeling and Theoretical Analysis for a Neighborhood-Scale Cool Roof Demonstration, 24, Urban Climate, 2018, pp. 616–632.
[29] A.D. Jayakaran, et al., Remediation of stormwater pollutants by porous asphalt pavement, Water. (Basel) 11 (3) (2019) 520.
[30] G.E. Kyriakodis, M. Santamouris, Using Reflective Pavements to Mitigate Urban Heat Island in Warm Climates - Results from a Large Scale Urban Mitigation Project, 24, Urban Climate, 2018, pp. 326–339.
[31] H. Li, et al., The use of reflective and permeable pavements as a potential practice for heat island mitigation and stormwater management, Environ. Res. Lett. 8 (1) (2013) 015023.
[32] M. Pomerantz, H. Akbari, J.T. Harvey, Cooler Reflective Pavements give Benefits Beyond Energy savings: Durability and Illumination, Lawrence Berkeley National Laboratory, 2000.
[33] S. Vujovic, et al., Urban Heat Island: causes, consequences, and mitigation measures with emphasis on reflective and permeable pavements, Civil. Eng. 2 (2) (2021) 459–484.
[34] A. Synnefa, et al., Experimental testing of cool colored thin layer asphalt and estimation of its potential to improve the urban microclimate, Build. Environ. 46 (1) (2011) 38–44.
[35] Kinouchi, T., et al., Development of cool pavement with dark colored high albedo coating, in 5th Conference for the Urban Environment. 2004.
[36] K. Hu, et al., Proposed cool coatings with high near-infrared reflectance and heat insulation for asphalt pavement, Coatings, 11 (1) (2021) 85.
[37] S. Stüwe, B. Hofko, Exploring cool pavement technologies: a lab-based experimental analysis of temperature and reflectivity, Transp. Res. Rec. 0 (0) (2024) 03611981241284624.
[38] A. Synnefa, M. Santamouris, I. Livada, A study of the thermal performance of reflective coatings for the urban environment, Sol. Energy 80 (8) (2006) 968–981.
[39] H. Li, J. Harvey, A. Kendall, Field measurement of albedo for different land cover materials and effects on thermal performance, Build. Environ. 59 (2013) 536–546.
[40] C. Ghenai, et al., Evaluation and thermal performance of cool pavement under desert weather conditions: surface albedo enhancement and carbon emissions offset, Case Stud. Constr. Mater. 18 (2023) e01940.
[41] M. Taleghani, U. Berardi, The Effect of Pavement Characteristics on pedestrians' Thermal Comfort in Toronto, 24, Urban Climate, 2018, pp. 449–459.
[42] R. Levinson, et al., Life-Cycle Assessment and Co-Benefits of Cool Pavements, Lawrence Berkeley National Laboratory, 2017.
[43] M. Pomerantz, et al., Examples of Cooler Reflective Streets for Urban Heat-Island mitigation: Portland cement Concrete and Chip Seals, Lawrence Berkeley National Laboratory, 2003.
[44] M. Pomerantz, et al., The Effect of pavements' Temperatures on Air Temperatures in Large Cities, Lawrence Berkeley National Laboratory, 2000.
[45] R.B. Mallick, et al., Pavement life–Extending potential of geosynthetic-reinforced chip seal with high-reflectivity aggregates, Transp. Res. Rec. 2474 (1) (2015) 19–29.
[46] J.J. Emery, et al., Light-coloured grey asphalt pavements: from theory to practice, Int. J. Pavement Eng. 15 (1) (2014) 23–35.
[47] E. Bühlmann, A.05 Synthese Kühle Strassenbeläge, Natl. Cent. Clim. Serv. (2021).
[48] Singer, T., et al., Teststrecke kühle Beläge Neue Murtenstrasse, Bern - monitoring Sommer 2020 bis 2024. 2025, Grolimund + Partner AG.
[49] N. Tran, et al., Strategies for design and construction of high-reflectance asphalt pavements, Transp. Res. Rec. 2098 (1) (2009) 124–130.
[50] Alleman, J. and M. Heitzman, Quantifying pavement albedo. 2019. p. 232.
[51] C. Richard, et al., Albedo of pavement surfacing materials, Situ Measuremets, in: 16th International Conference on Cold Regions Engineering, Salt Lake City, 2015.
[52] ASTM, Standard test method for measuring solar reflectance of horizontal and low-sloped surfaces in the field. 2021.
[53] J.S. Golden, K.E. Kaloush, Mesoscale and microscale evaluation of surface pavement impacts on the urban heat island effects, Int. J. Pavement Eng. 7 (1) (2006) 37–52.
[54] M. Martin, et al., Infrared thermography in the built environment: a multi-scale review, Renew. Sustain. Energy Rev. 165 (2022) 112540.
[55] MeteoSwiss. Available from: https://www.meteoswiss.admin.ch/services-and-publications/applications/ext/download-data-without-coding-skills.html#lang=en&mdt=normal&pgid=&sid=&col=&di=&tr=&hdr.
[56] L. Porot, et al., Recommendation of RILEM TC 237-SIB on affinity between aggregates and bituminous binders, Mater. Struct. 51 (6) (2018) 173.
[57] Y. Chen, K. Hu, S. Cao, Thermal performance of novel multilayer cool coatings for asphalt pavements, Materials. 12 (12) (2019) 1903.
[58] B. Yang, et al., Surface characteristics of ageing asphalt binder coupling thermal oxidation and ultraviolet radiation, Transp. Res. Rec. 2676 (10) (2022) 147–162.
[59] Global Solar Atlas. 2011 Annual average Global horizontal irradiance (GHI): egerkingen, Switzerland: 1195 kWh/m2. Phoenix, Arizona: 2126 kWh/m2. San Antonio, Texas: 1761 kWh/m2; Available from: https://globalsolaratlas.info/.
[60] Z. Chen, et al., Analysis of cooling performance and environmental benefit of asphalt pavement materials using light-colored aggregates, Constr. Build. Mater. 458 (2025) 139498.
[61] M.A. Khasawneh, et al., Thermal features prediction in asphalt pavements using ANFIS-based regression, Discov. Civ. Eng. 2 (1) (2025) 97.
[62] P. Xu, et al., Influence of the surface texture parameters of asphalt pavement on light reflection characteristics, Appl. Sci. 13 (23) (2023) 12824.
[63] S. Li, D. Harris, T. Wells, Surface texture and friction characteristics of diamond-ground concrete and asphalt pavements, J. Traffic Transp. Eng. Engl. Ed. 3 (5) (2016) 475–482.
[64] J.R. Marcobal, F. Salado, G. Flintsch, Evaluation of various surface cleaning techniques inside tunnels on pavement skid resistance, Materials 14 (19) (2021) 5660.
[65] M.T.A. Sarkar, et al., Influence of shotblasting treatment on asphalt pavement performance, Int. J. Pavement Eng. 23 (13) (2022) 4831–4844.